Flavor gauge bosons at the Fermilab Tevatron

Gustavo Burdman* and R. Sekhar Chivukula[†]
Department of Physics, Boston University, Boston, Massachusetts 02215

Nick Evans[‡]
Department of Physics, University of Southampton, Southampton, S017 1BJ, United Kingdom
(Received 12 May 2000; published 11 September 2000)

We investigate collider signals for gauged flavor symmetries that have been proposed in models of dynamical electroweak symmetry breaking and fermion mass generation. We consider the limits on the masses of the gauge bosons in these models which can be extracted from Fermilab Tevatron run I data in dijet production. Estimates of the run II search potential are provided. We show that the models also give rise to significant signals in single top quark production which may be visible at run II. In particular we study chiral quark family symmetry and SU(9) chiral flavor symmetry. The run I limits on the gauge bosons in these models lie between 1.5 and 2 TeV and should increase to about 3 TeV in run II. Finally, we show that an SU(12) enlargement of the SU(9) model, including leptonic interactions, is constrained by low energy atomic parity violation experiments to lie outside the reach of the Tevatron.

PACS number(s): 12.60.Cn, 12.60.Rc

I. INTRODUCTION

The origin of the standard model's (SM) familiar $SU(3)_c \times SU(2)_L \times U(1)_Y$ gauge symmetry remains theoretically unclear. In the limit where we neglect all gauge interactions and fermion masses, the fermion sector of the model possesses a large SU(45) global symmetry corresponding to the fact that in this limit there are 45 chiral fermion fields that are indistinguishable. The gauge interactions of the SM are by necessity subgroups of this maximal symmetry but in principle a larger subgroup of this symmetry might be gauged and broken to the SM groups at high energies.

Such gauged flavor symmetries have been invoked in a number of scenarios to play a role in the dynamical generation of fermion masses. For example they may play the part of extended technicolor [1] interactions in technicolor models [2] or top condensation models [3], feeding the electroweak symmetry (EWS) breaking fermion condensate down to provide masses for the lighter standard model fermions. Strongly interacting flavor gauge interactions may also be responsible for the condensation of the fermions directly involved in EWS breaking. For example, top condensation has been postulated to result from a top-color gauge group [4] and in the model of [5] from family gauge interactions. There has been renewed interest in these models recently with the realization that variants, in which the top quark mixes with singlet quarks, can give rise to both the EW scale and an acceptable top quark mass via a seesaw mass spectrum [6,7]. These top seesaw models have the added benefit of a decoupling limit which allows the presence of the singlet fields to be suppressed in precision EW measurements, bringing these dynamical models in line with the data. Flavor universal variants of the top-seesaw idea

have been proposed in Ref. [8], where the dynamics is driven by family or large flavor gauge symmetries.

The naive gauging of flavor symmetries at low scales (of order a few TeV) often gives rise to unacceptably large flavor changing neutral current (FCNC) since gauge and mass eigenstates need not coincide. For instance, gauge symmetries that give rise to direct contributions to K^0-$\bar{K}^0$ mixing are typically constrained to lie above 500 TeV in mass scale. There are, however, models that survive these constraints. Gauge groups that only act on the third family are less experimentally constrained—the top-color model [4] is such an example. Models in which the chiral flavor symmetries of the SM fermions are gauged preserving the SM $U(3)^5$ [9] flavor symmetry can respect the SM Glashow-Iliopoulos-Maiani (GIM) mechanism and do not give rise to tree level FCNC [10]. In addition, there are also strong constraints on gauged flavor models where the dynamics responsible for the breaking of the flavor symmetry does not respect custodial isospin [11]. We shall restrict ourselves to models where the top quark mass is the sole source of custodial isospin breaking. In particular we will study a model where the SU(3) chiral family symmetry of the quarks is gauged and another where the full SU(9) family-color multiplicity of the quarks is gauged, corresponding to the models of [8]. In the spirit of these models it is also interesting to consider chiral flavor symmetries that include the leptons which might be expected to give interesting contributions to Drell-Yan production. The obvious extension has a gauged SU(12) flavor symmetry but we show in the final section that an analysis of low energy atomic parity violation experiments places constraints on the gauge bosons of such models of the order of 10 TeV and they are thus outside the reach of the Tevatron.

Since these new flavor interactions may exist at relatively low scales (a few TeV) and may play an integral part in either EWS breaking or fermion mass generation it is interesting to study current experimental bounds on the corresponding gauge bosons. In a previous paper we investigated the limits from Z-pole precision measurements [12]. Al-

*Email address: burdman@bu.edu
[†]Email address: sekhar@bu.edu
[‡]Email address: n.evans@hep.phys.soton.ac.uk

though the limits obtained vary across models, the typical lower bound on the mass scale is 2 TeV. Here we study the potential of direct searches at the Fermilab Tevatron collider. In particular we study effects in dijet production (in the spirit of the analysis in [15,16]) and single top quark production. When possible, we first establish bounds from the existing run I data (they are typically 1–2 TeV). We then project the sensitivity of the Tevatron in run II and show the bounds are more than competitive with the precision data bounds. If these gauge symmetries do have a role to play in EWS breaking, then they must presumably be broken at scales close to the EW scale and these bounds therefore represent a significant probe of the interesting parameter space.

II. CONSTRAINTS ON MODELS

We present three models of flavoron physics. While this list is not exhaustive, we believe these examples cover a broad range of signals at the Fermilab Tevatron collider. In what follows, only the couplings to standard model fermions will be specified. Explicit models include additional fermions, necessary for either flavor gauge symmetry breaking and/or anomaly cancellation, which typically have masses of order of the flavor gauge symmetry breaking scale.

A. Chiral quark family symmetry

The gauging of the chiral family symmetry of the left handed quarks has been motivated in technicolor [10], top condensate [5] and flavor universal seesaw models [8]. The minimal representative model has a gauged SU(3) family symmetry, in addition to the SM interactions, acting on the three left handed quark[1] doublets Q $=((t,b)_L^i,(c,s)_L^i,(u,d)_L^i)$ where i is a QCD index which commutes with the family symmetry [8]. We assume that some massive sector completely breaks the SU(3) family gauge group to an global SU(3) family symmetry, giving the family gauge bosons ("familons") masses of order M_F $=g_F V$ where V is the mass scale associated with the symmetry breaking. There is no mixing between the flavor and standard model gauge bosons. Note that with this gauge symmetry and symmetry breaking pattern, the (approximate) SM $U(3)^5$ global symmetry responsible for the GIM mechanism [9] remains and the model is free of tree level FCNC [10]. The interactions of the massive flavorons are summarized by the couplings

$$\mathcal{L}=ig_F A^{\mu a}\bar{Q}\gamma_\mu T^a Q, \tag{1}$$

where T^a are the generators of SU(3) symmetry acting on the three families of left-handed quarks.

The SU(3) coupling g_F cannot be too large or this interaction will cause a chiral symmetry breaking condensate between the left-handed ordinary fermions and right-handed

fermions which must be present in the theory to eliminate gauge anomalies. This would result in TeV-scale fermion masses and a scale for electroweak symmetry breaking which is too high. We may estimate the upper bound on g_F by approximating, at low energies, the interactions of the massive flavor gauge bosons by a Nambu–Jona-Lasinio (NJL) model with the four-fermion interaction

$$\mathcal{L}_{eff}=-\frac{2\pi\kappa_F}{M_F^2}\left(\sum_f \bar{Q}\gamma_\mu T^a Q\right)^2, \tag{2}$$

where $\kappa\equiv g_F^2/4\pi$. Applying the usual NJL analysis,[2] we see that κ_F cannot exceed

$$\kappa_{crit}=\frac{2N\pi}{(N^2-1)}=2.36, \tag{3}$$

where $N=3$ for chiral quark flavor symmetry.

In Ref. [12] we obtained bounds on flavor gauge boson masses from electroweak precision measurements. The lower bound obtained for a critically coupled familon is M_F >1.9 TeV, at 95% C.L. Here we will investigate the reach of direct searches. First, we consider the bounds from the existing Tevatron data. As is the case for the universal coloron model [13], stringent limits will come from the study of the angular behavior of the dijet cross section [16]. The contributions arising in the chiral quark family model are the consequence of the exchange of the familon gauge boson in the various possible channels. The resulting modification of the quark scattering matrix elements are given in subsection 2 of the Appendix.

In Fig. 1 we plot the ratio of the dijet mass distribution for $|\eta|<0.5$ to the mass distribution with $0.5<|\eta|<1.0$, with η the jet pseudo-rapidity. This ratio, as noted for instance in Refs. [16,17], is very sensitive to new physics producing effects concentrated in the central region and in general affecting the angular distribution of dijets. Also it is expected that in this ratio there is a large cancellation of uncertainties coming from softer QCD effects. The uncertainty due to the choice of parton distribution functions is less than [17] 3%, and that coming from the choice of renormalization and factorization scale is about 6%.

The data points are from the D0 data in Ref. [17], and the error bars show the statistical and systematic errors added in quadrature. The histogram corresponds to the QCD prediction, obtained to next-to-leading order (NLO) with the use of JETRAD (see [16,17] for details). The familon contribution is known only at leading order (LO). Thus, in order to estimate their NLO dijet spectrum, we compute the fractional excess with respect to LO QCD and then multiply it by the NLO QCD result. We consider various familon masses, with the coupling set at its critical value.

---

[1] One can also imagine the same symmetry acting on leptons [8]. Here we only consider the quarks since they lead to signals at hadron colliders.

[2] Note that, defining the theory in terms of a momentum-space cutoff Λ, a four fermion interaction $G\bar{\psi}\psi\bar{\psi}\psi$ has a critical coupling $G_c=2\pi^2/\Lambda^2$ [14].
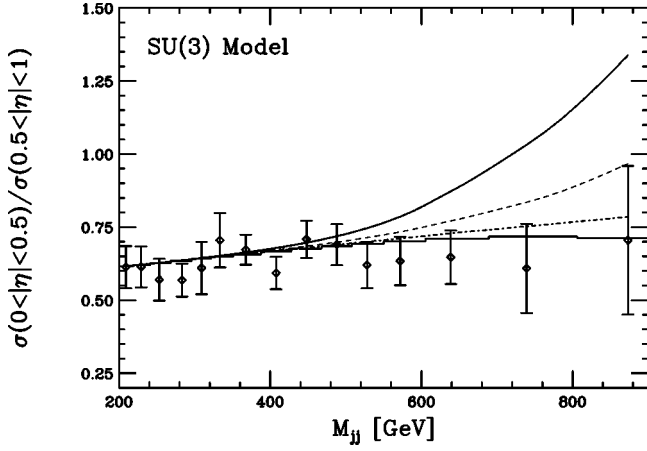
FIG. 1. The ratio of cross sections for $(|\eta|<0)/(0.5<|\eta|1.0)$ vs the dijet invariant mass, for the SU(3) chiral quark family model, for $M_F=1.2$ (solid lines), 1.5 (dashed line) and 2 TeV (dot-dashed line). The data points are from the D0 measurement [17], with the error bars including the statistical and systematic errors added in quadrature. The histogram is the NLO QCD prediction from JETRAD, using the CTEQ3M parton distribution function.

In order to obtain a lower mass limit we follow the procedure described in Ref. [16]. We construct the Gaussian likelihood function

$$P(x)=\frac{1}{2\pi^2\det(S)}\exp\left(-\frac{1}{2}[d-t(x)]^T S^{-1}[d-t(x)]\right),$$
(4)

where the vector d contains the data points in the various mass bins, $t(x)$ is the vector of theoretical predictions for a given mass and coupling $x=\kappa_F/M_F^2$, and S is the covariant matrix. To obtain 95% confidence level limits, we require

$$Q(x_{\max})\equiv\int_0^{x_{\max}}P(x)dx=0.95Q(\infty),$$
(5)

with $x_{\max}$ the value defining the mass bound. Making use of the run I data we then obtain mass bounds for the familon:

$$M_F>1.55 \quad \text{TeV}, \quad 95\% \text{ C.L.},$$
(6)

where we have considered a critically coupled familon. This is consistent with, but somewhat weaker than the 95% C.L. limit obtained in Ref. [12], $M_F>1.9$ TeV at critical coupling.

During run II, however, measurements of the dijet spectrum at an upgraded Tevatron will yield bounds better than those derived from Z-pole observables. For instance, if we consider the nominal luminosity of 2 fb^{-1} and assume a 30% reduction in the systematic errors, the bound on the familon mass for run II would be $M_F>2.2$ TeV. An extended Tevatron run or the achievement of higher intensities could therefore result in a mass reach well above that of electroweak precision measurements and cover a large fraction of the interesting parameter space of this model.
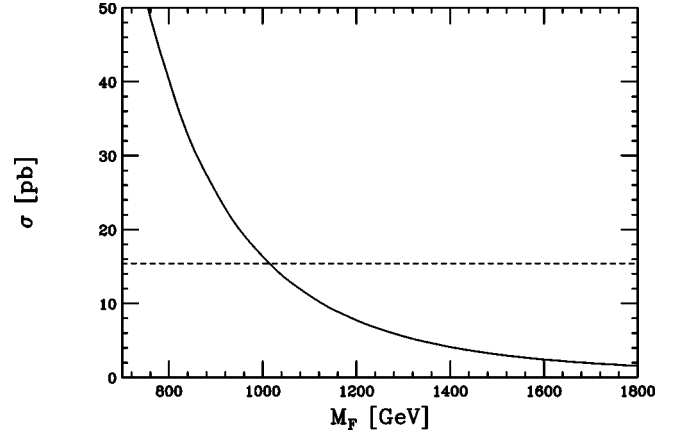

FIG. 2. Single top quark production cross section in the SU(3) family model vs the familon mass, at $\sqrt{s}=1.8$ TeV. The dashed horizontal line corresponds to the 95% C.L. bound from Ref. [18].

In addition to the dijet signal, the chiral quark family model leads to another potentially interesting signal at hadron colliders: anomalous single top quark production. This occurs due to the existence of non-diagonal couplings to the family gauge bosons. Although these do not lead to $|\Delta S|=2$ signals, because of GIM cancellation, there are flavor changing couplings of quarks. The fact that the family symmetry commutes with SU(2)$_L$ implies that there will be tree level familon exchanges such as $d\bar{b}\to u\bar{t}$, where "family number" is preserved. The diagrams relevant for single top quark production at the Tevatron are s-channel $d\bar{b}\to u\bar{t}$, and t-channel $u\bar{d}\to t\bar{b}$ (dominant) and $u\bar{b}\to t\bar{d}$. Other diagrams also are obtained by the replacements $d\to s$ and $u\to c$. For instance, the s-channel matrix element squared is

$$|\mathcal{M}(d\bar{b}\to u\bar{t})|^2=(4\pi)^2\kappa^2 u(u-m_t^2)\left|\frac{1}{2}P_s\right|^2.$$
(7)

Neglecting m_b, the t-channel contributions are obtained by replacing P_s by the P_t, where P_s and P_t are the familon propagators in the corresponding channel as defined in Eq. (A5). If the coupling is close to critical, these processes will generate important contributions to the single top quark production cross section. In Fig. 2 we show the familon induced single top quark production cross section at $\sqrt{s}=1.8$ TeV as a function of the familon mass. The horizontal line is the 95% C.L. upper limit on single top quark production as obtained by the Collider Detector at Fermilab (CDF) Collaboration [18]. The most constraining bound $\sigma(p\bar{p}\to tX)<15.4$ pb translates into the familon mass bound

$$M_F>1.02 \quad \text{TeV}, \quad 95\% \text{ C.L.}$$
(8)

This is somewhat weaker than the bound (6) obtained from the run I dijet data, but may be improved if a study exploiting the kinematic differences between the SM and the flavoron signals is undertaken.

In run II, the Tevatron will be sensitive to SM single top quark production via W-gluon fusion as well as the s-channel W^* exchange. The latter process can be separated from the
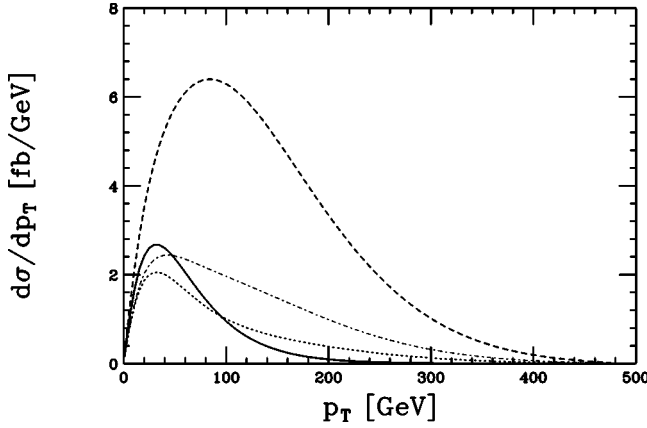
FIG. 3. The transverse momentum distribution in single top quark production in the SU(3) family model, for $\sqrt{s}=2$ TeV. Only the t-channel contribution, leading to the tb final state, is included. The solid line is the SM W^* s-channel process. The dashed line corresponds to $M_F=1.5$ TeV, the dot-dashed line to $M_F=2$ TeV and the dotted line to $M_F=2.5$ TeV.

former by making use of double b tagging, since the b quark produced in association with the top quark is hard, unlike in W-gluon fusion. In order to estimate the sensitivity of the Tevatron in run II to the flavoron contribution to single top quark production, we take only the dominant flavoron diagram, t-channel mediated $u\bar{d}\rightarrow t\bar{b}$. We compare this contribution to the s-channel SM, assuming these will be separately observed with the use of double b tagging [19]. In Fig. 3 we show the p_T distribution of the b quark produced in association with the top quark for t-channel familon exchange and s-channel W^* exchange. We see that, for example, for $M_F=2$ TeV the total ($t\bar{b}+\bar{t}b$) cross section is about 50% larger from familon exchange than in the SM, with the added feature that the p_T distribution is harder. We conclude that the sensitivity of run II could go as far as (2–2.5) TeV for 2 fb^{-1}, or perhaps higher depending on the sensitivity to be achieved to the SM s-channel process. Thus, anomalous single top quark production could be the most constraining channel on the SU(3) chiral quark model in run II at the Tevatron.

B. SU(9) chiral flavor symmetry

We next consider a natural extension of gauging the quark family symmetry, gauging the full SU(9) symmetry of both the color and family multiplicity of the left handed quarks. Such a symmetry can be implemented as an extended technicolor gauge symmetry (in the spirit of [20]) or in quark universal seesaw models (as in [8]). The SU(9) symmetry commutes with the standard weak SU(2)$_L$ gauge group and acts on the left handed quarks:

$$Q_L=((t,b)^r,(t,b)^b,(t,b)^g,(c,s)^r,\ldots(u,d)^g)_L \quad (9)$$

with r,g,b the three QCD colors. The quark couplings to the SU(9) gauge bosons is given by

$$\mathcal{L}=ig_F B^{a\mu}\bar{Q}_L\Lambda^a\gamma_\mu Q_L, \quad (10)$$

with Λ^a the generators of SU(9). These include

$$\frac{1}{\sqrt{3}}\begin{pmatrix} T^a & 0 & 0 \\ 0 & T^a & 0 \\ 0 & 0 & T^a \end{pmatrix}, \quad \frac{1}{\sqrt{6}}\begin{pmatrix} T^a & 0 & 0 \\ 0 & T^a & 0 \\ 0 & 0 & -2T^a \end{pmatrix},$$

$$\frac{1}{\sqrt{2}}\begin{pmatrix} T^a & 0 & 0 \\ 0 & -T^a & 0 \\ 0 & 0 & 0 \end{pmatrix}, \quad (11)$$

where T^a are the 8 3×3 QCD generators. SU(9) further contains

$$\frac{1}{\sqrt{2}}\begin{pmatrix} 0 & T^a & 0 \\ T^a & 0 & 0 \\ 0 & 0 & 0 \end{pmatrix}, \quad \frac{1}{\sqrt{12}}\begin{pmatrix} 0 & 1 & 0 \\ 1 & 0 & 0 \\ 0 & 0 & 0 \end{pmatrix},$$

$$\frac{1}{\sqrt{2}}\begin{pmatrix} 0 & -iT^a & 0 \\ iT^a & 0 & 0 \\ 0 & 0 & 0 \end{pmatrix}, \quad \frac{1}{\sqrt{12}}\begin{pmatrix} 0 & -i & 0 \\ i & 0 & 0 \\ 0 & 0 & 0 \end{pmatrix} \quad (12)$$

plus the two other similar sets mixing the remaining families. Finally there are two diagonal generators

$$\frac{1}{\sqrt{12}}\begin{pmatrix} 1 & 0 & 0 \\ 0 & -1 & 0 \\ 0 & 0 & 0 \end{pmatrix}, \quad \frac{1}{\sqrt{36}}\begin{pmatrix} 1 & 0 & 0 \\ 0 & 1 & 0 \\ 0 & 0 & -2 \end{pmatrix}. \quad (13)$$

The model must also contain interactions which give rise to color for the right handed quarks. For this reason, we include an SU(3)$_{pc}$ proto-color group that acts on the right handed quarks, which will be combined with the SU(3)$_C$ subgroup of SU(9)$_L$ to yield ordinary color. We normalize the proto-color gauge bosons couplings such that they have the same generators as the SU(9) bosons:

$$\mathcal{L}=\frac{i}{\sqrt{3}}g_{pc}A^{\mu a}\bar{q}_R\gamma_\mu T^a q_R. \quad (14)$$

At the flavor breaking scale we assume some massive sector breaks the SU(9)$_L\times$SU(3)$_{pc}$ gauge symmetry down to ordinary color SU(3)$_C$ and a global SU(3)$_F$ group acting on the three families of quarks. The global SU(3)$_F$ symmetry is sufficient to insure the absence of tree-level FCNC [20].

For simplicity, we will assume the symmetry breaking sector has an SU(9)$_L\times$SU(9)$_{flavor/color}$ chiral flavor symmetry, under which the symmetry breaking vacuum expectation value (VEV) transforms as a $(9,\bar{9})$. The majority of the SU(9) gauge bosons will then have mass $M_F=g_F V$. Eight of the SU(9)$_L$ gauge bosons mix with the right handed proto-color group, giving rise to ordinary color and eight massive gluons. The proto-gluons and color-octet flavorons mix through the mass matrix

$$(A^\mu, B^\mu) \begin{pmatrix} g_{pc}^2 & -g_{pc}g_F \\ -g_{pc}g_F & g_F^2 \end{pmatrix} V^2 \begin{pmatrix} A_\mu \\ B_\mu \end{pmatrix} \qquad (15)$$

which diagonalizes to

$$(X^\mu, G^\mu) \begin{pmatrix} g_{pc}^2 + g_F^2 & 0 \\ 0 & 0 \end{pmatrix} V^2 \begin{pmatrix} X_\mu \\ G_\mu \end{pmatrix} \qquad (16)$$

where

$$\begin{pmatrix} A^\mu \\ B^\mu \end{pmatrix} = \begin{pmatrix} \cos\phi & -\sin\phi \\ \sin\phi & \cos\phi \end{pmatrix} \begin{pmatrix} G_\mu \\ X_\mu \end{pmatrix} \qquad (17)$$

with

$$\sin\phi = \frac{g_{pc}}{\sqrt{g_{pc}^2 + g_F^2}}, \quad \cos\phi = \frac{g_F}{\sqrt{g_{pc}^2 + g_F^2}}, \qquad (18)$$

and G^μ and X^μ are the gluon and color-octet flavoron respectively.

The low energy QCD coupling, with the standard generator normalization is given by

$$g_c = \frac{g_F g_{pc}}{\sqrt{3(g_{pc}^2 + g_F^2)}} \qquad (19)$$

which implies that $\kappa_F \geq 3\alpha_s(2 \text{ TeV})$. The interactions of the SM fermions with the massive color octet (with mass $M_{F'} = \sqrt{g_{pc}^2 + g_F^2}V = M_F/c_\phi$) are given by

$$-g_c \tan\phi X^{a\mu} \bar{q}_R \gamma_\mu T^a q_R + g_c \cot\phi X^{a\mu} \bar{q}_L \gamma_\mu T^a q_L, \qquad (20)$$

where $\cot\phi = g_F/g_{pc}$.

As in the case of $SU(3)_F$, the coupling g_F cannot be too large, or it would likely induce an EWS breaking condensate at the flavor scale. Assuming that at low energies the massive gauge boson interactions with the SM fermions can be approximated by a NJL model (ignoring the effects of the mixing of eight of the generators with proto-color in this estimate), then the critical coupling for chiral symmetry breaking in that approximation is

$$\kappa_{crit} = \frac{2N\pi}{(N^2 - 1)} = 0.71. \qquad (21)$$

As was the case in the previous two models, the most conspicuous signals are in the dijet spectrum. In subsection 3 of the Appendix we list all the relevant matrix elements for dijet production due to the two gauge bosons with masses M_F and M_F'. In Fig. 4 we plot the contributions of these gauge bosons to the cross section ratio as a function of their mass, assuming for simplicity $M_F = M_F'$. Although, in principle, one could expect the effect to be smaller than for the SU(3) chiral familon due to the fact that the critical coupling in Eq. (21) is considerably smaller than that of the SU(3) case, the SU(9) flavorons contribute to a large number of diagrams, leading to dijets. In fact, as can be seen in Fig. 4,
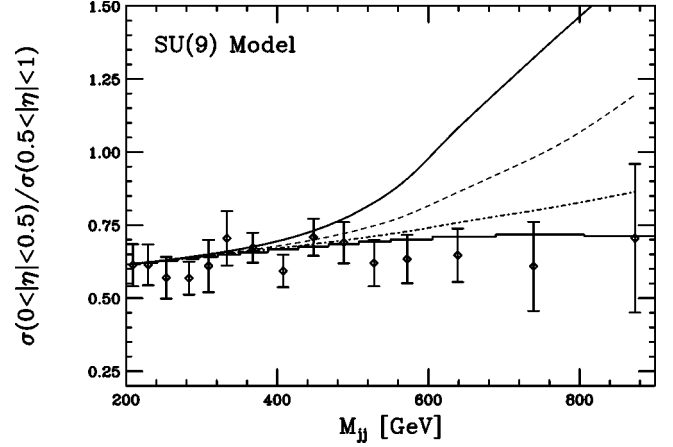

FIG. 4. The ratio of cross sections for $(|\eta| < 0.5)/(0.5 < |\eta| 1.0)$ vs the dijet invariant mass, for the SU(9) chiral flavor model, for $M_F = 1.2$ (solid lines), 1.5 (dashed lines) and 2 TeV (dot-dashed line). The data points are from the D0 measurement [17], with the error bars including the statistical and systematic errors added in quadrature. The histogram is the NLO QCD prediction from JETRAD, using the CTEQ3M parton distribution function.

the effects will be stronger in this model. We follow the procedure described earlier to obtain a mass constraint from the Tevatron run I data. The mass of the SU(9) flavorons is bounded by

$$M_F > 1.9 \text{ TeV}, \quad 95\% \text{ C.L.} \qquad (22)$$

This is very similar to the 95% C.L. limit obtained in Ref. [12] from electroweak precision measurements. On the other hand, at $\sqrt{s} = 2$ TeV and with an integrated luminosity of 2 fb^{-1}, run II at the Tevatron will put a limit of $M_F > 2.7$ TeV, where we assume a 30% reduction in systematic errors. This covers a large fraction of the interesting parameter space of this model.

Just as in the chiral quark family model, in the SU(9) model there are also important contributions to anomalous single top quark production. The fact that some of the SU(9) gauge bosons carry color tends to enhance the interactions when compared to the SU(3) chiral quark model. On the other hand, the critical coupling in this model is considerably smaller than that in the SU(3) case, as can be seen by comparing Eqs. (21) with (3). The net effect is a reduction in the single top quark signal shown in Fig. 3 by a factor of

$$\left(\frac{\kappa_F^{SU(9)}}{\kappa_F^{SU(3)}}\right)^2 \left(\frac{14}{9}\right) \simeq 0.15 \qquad (23)$$

at critical coupling. Since the cross section falls approximately as $1/M_F^4$, this will result in a familon mass bound that is smaller than the one to be obtained in the SU(3) model by a factor of about $\sqrt[4]{0.15} \simeq 0.60$. Thus, since our expectations for run II in the single top quark channel in the SU(3) model put the reach somewhere around $M_F > (2$–$2.5)$ TeV, we conclude that the reach of this channel for the SU(9) flavoron is still below the run I mass limit, Eq. (22), that we extracted from the dijet data. Although more detailed studies of the

single top quark signal (for instance including all possible single top quark final states) are possible, we can safely conclude that this channel will not be competitive with the dijet signal in the SU(9) model at the Tevatron.

C. SU(12) chiral flavor symmetry

The final model we consider is one in which we gauge the full SU(12) flavor symmetry of all the left handed SM fermion doublets [20,8]:

$$Q_L = ((t,b)^r, (t,b)^b, (t,b)^g, (\nu_\tau, \tau), (c,s)^r, \ldots (\nu_e, e))_L. \tag{24}$$

This is similar to the SU(9) model, but it also includes a proto-hypercharge interaction that, after the SU(12) breaking, gives rise to the SM U(1)$_Y$. The flavor gauge interactions act as

$$\mathcal{L} = i g_F B^{a\mu} \bar{Q}_L \Lambda^a \gamma_\mu Q_L, \tag{25}$$

with Λ^a the generators of SU(12), which may be conveniently broken down into the following groupings:

$$\frac{1}{\sqrt{3}} \begin{pmatrix} P^a & 0 & 0 \\ 0 & P^a & 0 \\ 0 & 0 & P^a \end{pmatrix}, \quad \frac{1}{\sqrt{6}} \begin{pmatrix} P^a & 0 & 0 \\ 0 & P^a & 0 \\ 0 & 0 & -2P^a \end{pmatrix},$$

$$\frac{1}{\sqrt{2}} \begin{pmatrix} P^a & 0 & 0 \\ 0 & -P^a & 0 \\ 0 & 0 & 0 \end{pmatrix} \tag{26}$$

where P^a are the 15 4×4 Pati-Salam generators consisting of 8 3×3 blocks that are QCD, 6 step operators between the quarks and leptons and the diagonal generator $1/\sqrt{24}$ diag$(1,1,1,-3)$. SU(12) further contains

$$\frac{1}{\sqrt{2}} \begin{pmatrix} 0 & P^a & 0 \\ P^a & 0 & 0 \\ 0 & 0 & 0 \end{pmatrix}, \quad \frac{1}{\sqrt{16}} \begin{pmatrix} 0 & 1 & 0 \\ 1 & 0 & 0 \\ 0 & 0 & 0 \end{pmatrix},$$

$$\frac{1}{\sqrt{2}} \begin{pmatrix} 0 & -iP^a & 0 \\ iP^a & 0 & 0 \\ 0 & 0 & 0 \end{pmatrix}, \quad \frac{1}{\sqrt{16}} \begin{pmatrix} 0 & -i & 0 \\ i & 0 & 0 \\ 0 & 0 & 0 \end{pmatrix} \tag{27}$$

plus the two other similar sets mixing the remaining families. Finally there are two diagonal generators

$$\frac{1}{\sqrt{16}} \begin{pmatrix} 1 & 0 & 0 \\ 0 & -1 & 0 \\ 0 & 0 & 0 \end{pmatrix}, \quad \frac{1}{\sqrt{48}} \begin{pmatrix} 1 & 0 & 0 \\ 0 & 1 & 0 \\ 0 & 0 & -2 \end{pmatrix}. \tag{28}$$

In order to ensure the SM gauge groups emerge at low energies we must again introduce a proto-color group as in the SU(9) model above. The first 8 generators of SU(12) in Eq. (26) are the same as those in the SU(9) model (11) and hence the discussion of the mixing between the proto-color and the

8 SU(12) gauge bosons follows the discussion in the SU(9) model exactly. In addition, in the SU(12) model we must also include a proto-hypercolor gauge boson. Since the Pati-Salam diagonal generator in the first set of generators in Eq. (26) is the traditional generator for the hypercharge boson's coupling to left handed fermions, the proto-hypercharge gauge boson only has to couple to the right handed fermions. The result of the mixing of these two gauge bosons is the massless SM hypercharge gauge boson plus a massive gauge boson coupling to both left and right handed fermions.

If the interactions of flavoron gauge bosons in Eq. (25) at low energies can be modeled by a NJL Lagrangian with coupling $4\pi\kappa/2!M_F^2$, the critical coupling for chiral symmetry breaking is calculated to be

$$\kappa_{crit} = \frac{2N\pi}{(N^2-1)} = 0.53, \tag{29}$$

somewhat smaller than in the SU(9) case in Eq. (21). Note that combined with the lower constraint from the ability to reproduce the QCD coupling $[\kappa_F \gtrsim 3\alpha_s(2\text{ TeV}) \simeq 0.3]$ there is a relatively small window of allowed couplings.

Although this model results in various signals at the Tevatron — such as quark scatterings similar to those of the SU(9) model as well as anomalous contributions to Drell-Yan production arising from the flavoron couplings to leptons — the energy scale of this scenario is severely constrained by data from experiments of atomic parity violation (APV) in cesium. The parity-violating part of the electron-nucleon interaction can be written as

$$\mathcal{L}_{eq} = \frac{G_F}{\sqrt{2}} \sum_{q=u,d} \{C_{1q}(\bar{e}\gamma_\mu\gamma_5 e)(\bar{q}\gamma^\mu q) + C_{2q}(\bar{e}\gamma_\mu e) \\ \times (\bar{q}\gamma^\mu\gamma_5 q)\}, \tag{30}$$

where the coefficients C_{1q} and C_{2q} are given in the SM by

$$C_{1q}^{SM} = -(T_3^q - 2Q_q\sin^2\theta), \quad C_{2q}^{SM} = -T_3^q(1 - 4\sin^2\theta), \tag{31}$$

and T_3^q is the third component of the quark isospin. The atomic weak charge is then defined as

$$Q_W = -2\{C_{1u}(2Z+N) + C_{1d}(N+2Z)\}, \tag{32}$$

with Z and N the number of protons and neutrons respectively. The APV experiment finds the atomic charge of cesium to be [21] $Q_W = -72.06 \pm 0.28 \pm 0.34$, whereas the SM prediction [22] is $Q_W = -73.09 \pm 0.03$. This translates into a deviation from the SM prediction of

$$\Delta Q_W = 1.33 \pm 0.44. \tag{33}$$

We can write the deviations of Q_W as

$$\Delta Q_W = -376\Delta C_{1u} - 422\Delta C_{1d}. \tag{34}$$

The SU(12) model gives rise to various contributions to ΔQ_W. However, by far the largest of these corresponds to a

step operator from the generators in Eq. (26) which connect quarks to leptons. These result in the non-diagonal effective coupling

$$-\frac{g_F^2}{8\,M_F^2}(\bar{e}_L\gamma_\mu d_L)(\bar{d}_L\gamma^\mu e_L). \tag{35}$$

After Fierzing and decomposing into the proper vector and axial vector pieces, the contribution in Eq. (35) gives rise to an effect in the weak charge of cesium given by

$$\Delta Q_W^F = -80.4\kappa_F\frac{(1\text{ TeV})^2}{M_F^2} = -42.6\frac{(1\text{ TeV})^2}{M_F^2}, \tag{36}$$

where M_F is understood to be measured in TeV, and the last equality is obtained by using $\kappa_F = \kappa_{\text{crit}}$ as defined in Eq. (29). Thus not only is this a *large* contribution to $Q_W(Cs)$, but it also has the opposite sign of Eq. (33). For instance, the 3σ bound would be $M_F > 12$ TeV. More conservatively, we can estimate the sensitivity of the APV measurement by taking the error in Eq. (33) as the possible size of the effect. This translates into $M_F > 9.8$ TeV. From the model building point of view this is an undesirably large mass scale and raises the issue of fine-tuning. In any event, it is clear that the APV experiment forces the mass scale in the SU(12) model to be very high and out of reach of the Tevatron.

Finally, we point out that the constraint on the SU(12) model resulting from Eq. (36) is more general since it cannot be completely evaded by lowering the coupling below its critical value. As we mentioned earlier, in order to obtain the correct QCD coupling, κ_F must satisfy $\kappa_F \geqslant 3\alpha_s(2\text{ TeV})$. Then, its minimum value of approximately 0.3 translates into the bound $M_F > 7.4$ TeV.

III. CONCLUSIONS

We have studied the Tevatron collider bounds on two models of broken, gauged, chiral flavor symmetries: an SU(3) chiral family symmetry and an SU(9) chiral flavor symmetry of the SM quarks. These symmetries have been proposed as playing a significant role in theories of EWS breaking and fermion mass generation and are blessed with a GIM mechanism that suppresses FCNC, allowing the gauge bosons to be relatively light. The strongest Tevatron signals result in dijet production and single top quark production. We summarize the current limits, from precision data [12] and run I, on the critically coupled gauge boson masses in Table I—they are comparable. The run II expectations are also displayed and should become the leading constraints on the models.

In the SU(3) model both, dijet and anomalous single top quark production, are likely to be important signals. On the other hand, in the SU(9) model the dijet cross section receives a large enhancement due to the fact that some of the flavor gauge bosons carry color, resulting in more diagrams contributing (see subsection 3 of the Appendix). However, since the critical coupling is considerably smaller than in the SU(3) case, the single top quark signal—even after taking into account the color enhancement—is reduced. Thus, the

TABLE I. The 95% C.L. bounds (or sensitivity) on the models discussed. The numbers correspond to the mass of the gauge bosons in TeV if its coupling is critical. The first column comes from electroweak precision measurements and is taken from Ref. [12]. The run I bounds as well as the run II sensitivities (for 2 fb^{-1}) summarize our results. They come from the dijet analysis, with the exception of the run II reach for the SU(3) chiral quark model which comes from single top quark production.

	EPM	Run I	Run II
Universal coloron	3	4.3	7
SU(3)$_F$	1.9	1.55	2.5 (single top quark)
SU(9)$_F$	1.9	1.9	2.7
SU(12)$_F$	10 (APV)	No reach	No reach

single top quark channel is crucial in order to separate these two models as the possible origin of a hypothetical deviation in the dijet sample.

For comparison we also display in Table I the equivalent limits for the universal coloron model of [15,16]—in this model the chiral SU(3)$_L \times$ SU(3)$_R$ color group of the quarks is gauged and broken to the QCD group, leaving axially coupling massive colorons. This model is considerably more strongly constrained in part because of its large critical coupling and because the dijet channel is a particularly good probe of extra color-like interactions. It is notable that in the models we have explored the gauge bosons are potentially lighter, as one might hope if they played a role in EWS breaking, and that the Tevatron can hope to probe interesting regions of parameter space.

Finally we have pointed out a further low energy precision constraint on models where the flavor symmetry is enlarged to include the lepton sector. In particular an SU(12) gauged chiral flavor model gives contributions in low energy atomic parity violation experiments that place the bound on the gauge boson masses out of the Tevatron's reach.

APPENDIX: CROSS SECTIONS

We present some standard tree-level expressions for cross sections:

$$\frac{d\sigma}{dt} = \frac{1}{16\pi}\frac{1}{s^2}|\mathcal{M}|^2. \tag{A1}$$

To obtain the full cross section we must average over initial states and sum over final states. Summing over spins and splitting the matrix element into chiral components we have

$$\bar{L}L \to \bar{L}L: \quad \frac{1}{4}\sum_{spin}|\mathcal{M}|^2 = u^2\left|\sum_i P_iQ_i\right|^2 \quad \text{(A2)}$$

$$\bar{L}R \to \bar{L}R: \quad \frac{1}{4}\sum_{spin}|\mathcal{M}|^2 = s^2\left|\sum_i P_iQ_i\right|^2 \quad \text{(A3)}$$

$$\bar{L}L \to \bar{R}R: \quad \frac{1}{4}\sum_{spin}|\mathcal{M}|^2 = t^2\left|\sum_i P_iQ_i\right|^2 \quad \text{(A4)}$$

where P_i is the propagator factor associated with each diagram taking the form

$$P_i = \frac{-i}{q_i^2 - M_F^2 + i\Gamma_F M_F} \quad \text{(A5)}$$

and one must sum over all gauge bosons and $q_i^2 = s, t$ channels. Q_i are the group theory factors associated with each diagram. Application of the above construction kit, averaging over initial color states (1/9) and summing final color states gives the QCD backgrounds and flavor model contributions to dijet processes.

1. QCD backgrounds

The QCD contributions to the dijet cross section are

$$\frac{d\sigma}{dt}(qq \to qq) = \frac{4\pi\alpha_s^2}{9s^2}\left(\frac{u^2+s^2}{t^2} + \frac{t^2+s^2}{u^2} - \frac{2}{3}\frac{s^2}{ut}\right) \quad \text{(A6)}$$

$$\frac{d\sigma}{dt}(q\tilde{q} \to q\tilde{q}) = \frac{4\pi\alpha_s^2}{9s^2}\left(\frac{s^2+u^2}{t^2}\right) \quad \text{(A7)}$$

$$\frac{d\sigma}{dt}(q\bar{q} \to \tilde{q}\bar{\tilde{q}}) = \frac{4\pi\alpha_s^2}{9s^4}(t^2+u^2) \quad \text{(A8)}$$

$$\frac{d\sigma}{dt}(q\bar{q} \to q\bar{q}) = \frac{4\pi\alpha_s^2}{9s^2}\left(\frac{s^2+u^2}{t^2} + \frac{t^2+u^2}{s^2} - \frac{2}{3}\frac{u^2}{st}\right) \quad \text{(A9)}$$

$$\frac{d\sigma}{dt}(q\bar{\tilde{q}} \to q\bar{\tilde{q}}) = \frac{4\pi\alpha_s^2}{9s^s}\left(\frac{s^2+u^2}{t^2}\right) \quad \text{(A10)}$$

$$\frac{d\sigma}{dt}(gg \to q\bar{q}) = \frac{\pi\alpha_s^2}{6s^2}\left(\frac{u}{t} + \frac{t}{u} - \frac{9}{4}\frac{t^2+u^2}{s^2}\right) \quad \text{(A11)}$$

$$\frac{d\sigma}{dt}(q\bar{q} \to gg) = \frac{32\pi\alpha_s^2}{27s^2}\left(\frac{u}{t} + \frac{t}{u} - \frac{9}{4}\frac{t^2+u^2}{s^2}\right) \quad \text{(A12)}$$

$$\frac{d\sigma}{dt}(qg \to qg) = \frac{4\pi\alpha_s^2}{9s^2}\left(-\frac{u}{s} - \frac{s}{u} + \frac{9}{4}\frac{s^2+u^2}{t^2}\right) \quad \text{(A13)}$$

$$\frac{d\sigma}{dt}(gg \to gg) = \frac{9\pi\alpha_s^2}{2s^2}\left(3 - \frac{tu}{s^2} - \frac{su}{t^2} - \frac{st}{u^2}\right). \quad \text{(A14)}$$

2. Chiral quark family symmetry: Matrix elements into dijets

The squared matrix elements in the model of Sec. II A, including the interference with QCD:

$$\Delta|\mathcal{M}(qq \to qq)|^2 = (4\pi)^2\kappa^2 s^2\left|\frac{1}{3}P_t - \frac{1}{3}P_u\right|^2$$
$$- \frac{(4\pi)^2\kappa\alpha_s s^2}{9}\text{Re}\left(\frac{1}{t}P_t + \frac{1}{u}P_u - \frac{1}{u}P_t\right.$$
$$\left. - \frac{1}{t}P_u\right) \quad \text{(A15)}$$

$$\Delta|\mathcal{M}(ud \to ud)|^2 = \frac{(4\pi)^2\kappa^2 s^2}{9}|P_t|^2$$
$$+ \frac{(4\pi)^2\kappa\alpha_s s^2}{9}\text{Re}\left(\frac{1}{t}P_t\right) \quad \text{(A16)}$$

$$\Delta|\mathcal{M}(us \to us)|^2 = \frac{(4\pi)^2\kappa^2 s^2}{36}|P_t|^2$$
$$+ \frac{(4\pi)^2\kappa\alpha_s s^2}{18}\text{Re}\left(\frac{1}{t}P_t\right) \quad \text{(A17)}$$

$$\Delta|\mathcal{M}(ds \to ds)|^2 = (4\pi)^2\kappa^2 s^2\left|\frac{1}{6}P_t + \frac{1}{2}P_u\right|^2$$
$$+ \frac{(4\pi)^2\kappa\alpha_s s^2}{3}\text{Re}\left(\frac{1}{6t}P_t + \frac{1}{2t}P_u\right) \quad \text{(A18)}$$

$$\Delta|\mathcal{M}(q\bar{q} \to q\bar{q})|^2 = (4\pi)^2\kappa^2 u^2\left|\frac{1}{3}P_t - \frac{1}{3}P_s\right|^2$$
$$- \frac{(4\pi)^2\kappa\alpha_s u^2}{9}\text{Re}\left(\frac{1}{s}P_t + \frac{1}{t}P_s\right) \quad \text{(A19)}$$

$$\Delta|\mathcal{M}(u\bar{u} \to d\bar{d})|^2 = (4\pi)^2\kappa^2 u^2\left|\frac{1}{3}P_s\right|^2 \quad \text{(A20)}$$

$$\Delta|\mathcal{M}(u\bar{u} \to s\bar{s})|^2 = (4\pi)^2\kappa^2 u^2\left|\frac{1}{6}P_s\right|^2 \quad \text{(A21)}$$

$$\Delta|\mathcal{M}(d\bar{d} \to s\bar{s})|^2 = (4\pi)^2\kappa^2 u^2\left|\frac{1}{6}P_s + \frac{1}{2}P_t\right|^2$$
$$- \frac{(4\pi)^2\kappa\alpha_s u^2}{6}\text{Re}\left(\frac{1}{s}P_t\right) \quad \text{(A22)}$$

$$\Delta|\mathcal{M}(s\bar{d} \to s\bar{d})|^2 = (4\pi)^2\kappa^2 u^2\left|\frac{1}{2}P_s + \frac{1}{6}P_t\right|^2$$
$$- \frac{(4\pi)^2\kappa\alpha_s u^2}{6}\text{Re}\left(\frac{1}{t}P_s\right) \quad \text{(A23)}$$

$$\Delta|\mathcal{M}(u\bar{d} \to u\bar{d})|^2 = (4\pi)^2\kappa^2 u^2\left|\frac{1}{3}P_t\right|^2 \quad \text{(A24)}$$

$$\Delta|\mathcal{M}(u\bar{s} \to u\bar{s})|^2 = (4\pi)^2\kappa^2 u^2\left|\frac{1}{6}P_t\right|^2, \quad \text{(A25)}$$

where P_s, P_t and P_u are defined by Eq. (A5) and basically reflect the gauge boson propagator in the appropriate channel. Among the familon contributions we also include the interference with the gluon.

3. SU(9) chiral flavor symmetry: Matrix elements into dijets

The squared matrix elements, including QCD and the SU(9) model contributions, are:

$$|\mathcal{M}(q_L q_L \rightarrow q_L q_L)|^2 = \frac{2(4\pi)^2 s^2}{9}\left\{\left|\frac{\alpha_s}{t} + \frac{2\kappa}{3}P_t^F + \alpha_s\cot^2\phi P_t^{F'}\right|^2 + \left|\frac{\alpha_s}{u} + \frac{2\kappa}{3}P_u^F + \alpha_s\cot^2\phi P_u^{F'}\right|^2\right.$$
$$\left. - \frac{2}{3}\mathrm{Re}\left[\left(\frac{\alpha_s}{t} + \frac{2\kappa}{3}P_t^F + \alpha_s\cot^2\phi P_t^{F'}\right)\left(\frac{\alpha_s}{u} + \frac{2\kappa}{3}P_u^F + \alpha_s\cot^2\phi P_u^{F'}\right)\right]\right\} \tag{A26}$$

$$|\mathcal{M}(q_R q_R \rightarrow q_R q_R)|^2 = \frac{2(4\pi)^2 s^2}{9}\left\{\left|\frac{\alpha_s}{t} + \alpha_s\tan^2\phi P_t^{F'}\right|^2 + \left|\frac{\alpha_s}{u} + \alpha_s\tan^2\phi P_u^{F'}\right|^2\right.$$
$$\left. - \frac{2}{3}\mathrm{Re}\left[\left(\frac{\alpha_s}{u} + \alpha_s\tan^2\phi P_u^{F'}\right)\left(\frac{\alpha_s}{t} + \alpha_s\tan^2\phi P_t^{F'}\right)\right]\right\} \tag{A27}$$

$$|\mathcal{M}(q_L q_R \rightarrow q_L q_R)|^2 = \frac{2(4\pi)^2 u^2}{9}\left|\frac{\alpha_s}{t} - \alpha_s P_t^{F'}\right|^2 \tag{A28}$$

$$|\mathcal{M}(q_L q_R \rightarrow q_R q_L)|^2 = \frac{2(4\pi)^2 t^2}{9}\left|\frac{\alpha_s}{u} - \alpha_s P_u^{F'}\right|^2 \tag{A29}$$

$$|\mathcal{M}(u_L d_L \rightarrow u_L d_L)|^2 = \frac{2(4\pi)^2 s^2}{9}\left|\frac{\alpha_s}{t} + \frac{2\kappa}{3}P_t^F + \alpha_s\cot^2\phi P_t^{F'}\right|^2 \tag{A30}$$

$$|\mathcal{M}(u_R d_R \rightarrow u_R d_R)|^2 = \frac{2(4\pi)^2 s^2}{9}\left|\frac{\alpha_s}{t} + \alpha_s\tan^2\phi P_t^{F'}\right|^2 \tag{A31}$$

$$|\mathcal{M}(u_L d_R \rightarrow u_L d_R)|^2 = |\mathcal{M}(u_R d_L \rightarrow u_R d_L)|^2 = \frac{2(4\pi)^2 u^2}{9}\left|\frac{\alpha_s}{t} - \alpha_s P_t^{F'}\right|^2 \tag{A32}$$

$$|\mathcal{M}(u_L s_L \rightarrow u_L s_L)|^2 = \frac{2(4\pi)^2 s^2}{9}\left|\frac{\alpha_s}{t} - \frac{\kappa}{3}P_t^F + \alpha_s\cot^2\phi P_t^{F'}\right|^2 \tag{A33}$$

$$|\mathcal{M}(u_R s_R \rightarrow u_R s_R)|^2 = \frac{2(4\pi)^2 s^2}{9}\left|\frac{\alpha_s}{t} + \alpha_s\tan^2\phi P_t^{F'}\right|^2 \tag{A34}$$

$$|\mathcal{M}(u_L s_R \rightarrow u_L s_R)|^2 = |\mathcal{M}(u_R s_L \rightarrow u_R s_L)|^2 = \frac{2(4\pi)^2 u^2}{9}\left|\frac{\alpha_s}{t} - \alpha_s P_t^{F'}\right|^2 \tag{A35}$$

$$|\mathcal{M}(d_L s_L \rightarrow d_L s_L)|^2 = \frac{2(4\pi)^2 s^2}{9}\left\{\left|\frac{\alpha_s}{t} - \frac{\kappa}{3}P_t^F + \alpha_s\cot^2\phi P_t^{F'}\right|^2 + |\kappa P_s^F|^2\right.$$
$$\left. - \frac{2}{3}\mathrm{Re}\left[\kappa P_s^F\left(\frac{\alpha_s}{t} - \frac{\kappa}{3}P_t^F + \alpha_s\cot^2\phi P_t^{F'}\right)\right]\right\} \tag{A36}$$

$$|\mathcal{M}(d_R s_R \rightarrow d_R s_R)|^2 = \frac{2(4\pi)^2 s^2}{9}\left|\frac{\alpha_s}{t} + \alpha_s\tan^2\phi P_t^{F'}\right|^2 \tag{A37}$$

$$|\mathcal{M}(d_L s_R \rightarrow d_L s_R)|^2 = |\mathcal{M}(d_R s_L \rightarrow d_R s_L)|^2 = \frac{2(4\pi)^2 u^2}{9}\left|\frac{\alpha_s}{t} - \alpha_s P_t^{F'}\right|^2 \tag{A38}$$

$$|\mathcal{M}(q_L\bar{q}_L \to q_L\bar{q}_L)|^2 = \frac{2(4\pi)^2 u^2}{9}\left\{\left|\frac{\alpha_s}{s}+\frac{2\kappa}{3}P_s^F+\alpha_s\cot^2\phi P_s^{F'}\right|^2 + \left|\frac{\alpha_s}{t}+\frac{2\kappa}{3}P_t^F+\alpha_s\cot^2\phi P_t^{F'}\right|^2\right.$$
$$\left. -\frac{2}{3}\mathrm{Re}\left[\left(\frac{\alpha_s}{s}+\frac{2\kappa}{3}P_s^F+\alpha_s\cot^2\phi P_s^{F'}\right)\left(\frac{\alpha_s}{t}+\frac{2\kappa}{3}P_t^F+\alpha_s\cot^2\phi P_t^{F'}\right)\right]\right\} \tag{A39}$$

$$|\mathcal{M}(q_R\bar{q}_R \to q_R\bar{q}_R)|^2 = \frac{2(4\pi)^2 u^2}{9}\left\{\left|\frac{\alpha_s}{s}+\alpha_s\tan^2\phi P_s^{F'}\right|^2 + \left|\frac{\alpha_s}{t}+\alpha_s\tan^2\phi P_t^{F'}\right|^2\right.$$
$$\left. -\frac{2}{3}\mathrm{Re}\left[\left(\frac{\alpha_s}{s}+\alpha_s\tan^2\phi P_s^{F'}\right)\left(\frac{\alpha_s}{t}+\alpha_s\tan^2\phi P_t^{F'}\right)\right]\right\} \tag{A40}$$

$$|\mathcal{M}(q_L\bar{q}_L \to q_R\bar{q}_R)|^2 = |\mathcal{M}(q_R\bar{q}_R \to q_L\bar{q}_L)|^2 = \frac{2(4\pi)^2 t^2}{9}\left|\frac{\alpha_s}{s}-\alpha_s P_s^{F'}\right|^2 \tag{A41}$$

$$|\mathcal{M}(q_L\bar{q}_R \to q_L\bar{q}_R)|^2 = |\mathcal{M}(q_R\bar{q}_L \to q_R\bar{q}_L)|^2 = \frac{2(4\pi)^2 s^2}{9}\left|\frac{\alpha_s}{t}-\alpha_s P_t^{F'}\right|^2 \tag{A42}$$

$$|\mathcal{M}(u_L\bar{u}_L \to d_L\bar{d}_L)|^2 = \frac{2(4\pi)^2 u^2}{9}\left|\frac{\alpha_s}{s}+\frac{2\kappa}{3}P_s^F+\alpha_s\cot^2\phi P_s^{F'}\right|^2 \tag{A43}$$

$$|\mathcal{M}(u_R\bar{u}_R \to d_R\bar{d}_R)|^2 = \frac{2(4\pi)^2 u^2}{9}\left|\frac{\alpha_s}{s}+\alpha_s\cot^2\phi P_s^{F'}\right|^2 \tag{A44}$$

$$|\mathcal{M}(u_L\bar{u}_L \to d_R\bar{d}_R)|^2 = |\mathcal{M}(u_R\bar{u}_R \to d_L\bar{d}_L)|^2 = \frac{2(4\pi)^2 t^2}{9}\left|\frac{\alpha_s}{s}-\alpha_s P_s^{F'}\right|^2 \tag{A45}$$

$$|\mathcal{M}(u_L\bar{u}_L \to s_L\bar{s}_L)|^2 = \frac{2(4\pi)^2 u^2}{9}\left|\frac{\alpha_s}{s}-\frac{\kappa}{3}P_s^F+\alpha_s\cot^2\phi P_s^{F'}\right|^2 \tag{A46}$$

$$|\mathcal{M}(u_R\bar{u}_R \to s_R\bar{s}_R)|^2 = \frac{2(4\pi)^2 u^2}{9}\left|\frac{\alpha_s}{s}+\alpha_s\tan^2\phi P_s^{F'}\right|^2 \tag{A47}$$

$$|\mathcal{M}(u_L\bar{u}_L \to s_R\bar{s}_R)|^2 = |\mathcal{M}(u_R\bar{u}_R \to s_L\bar{s}_L)|^2 = \frac{2(4\pi)^2 t^2}{9}\left|\frac{\alpha_s}{s}-\alpha_s P_s^{F'}\right|^2 \tag{A48}$$

$$|\mathcal{M}(d_L\bar{d}_L \to s_L\bar{s}_L)|^2 = \frac{2(4\pi)^2 u^2}{9}\left\{\left|\frac{\alpha_s}{s}-\frac{\kappa}{3}P_s^F+\alpha_s\cot^2\phi P_s^{F'}\right|^2 + \frac{1}{2}|\kappa P_t^F|^2\right.$$
$$\left. -\frac{1}{3}\mathrm{Re}\left[\left(\frac{\alpha_s}{s}-\frac{\kappa}{3}P_s^F+\alpha_s\cot^2\phi P_s^{F'}\right)\kappa P_t^F\right]\right\} \tag{A49}$$

$$|\mathcal{M}(d_R\bar{d}_R \to s_R\bar{s}_R)|^2 = \frac{2(4\pi)^2 u^2}{9}\left|\frac{\alpha_s}{s}+\alpha_s\tan^2\phi P_s^{F'}\right|^2 \tag{A50}$$

$$|\mathcal{M}(d_L\bar{d}_L \to s_R\bar{s}_R)|^2 = |\mathcal{M}(d_R\bar{d}_R \to s_L\bar{s}_L)|^2 = \frac{2(4\pi)^2 t^2}{9}\left|\frac{\alpha_s}{s}-\alpha_s P_s^{F'}\right|^2 \tag{A51}$$

$$|\mathcal{M}(s_L\bar{d}_L \to s_L\bar{d}_L)|^2 = \frac{2(4\pi)^2 u^2}{9}\left\{\left|\frac{\alpha_s}{t}-\frac{\kappa}{3}P_t^F+\alpha_s\cot^2\phi P_t^{F'}\right|^2 + \frac{1}{2}|\kappa P_s^F|^2\right.$$
$$\left. -\frac{1}{3}\mathrm{Re}\left[\kappa P_s^F\left(\frac{\alpha_s}{t}-\frac{\kappa}{3}P_t^F+\alpha_s\cot^2\phi P_t^{F'}\right)\right]\right\} \tag{A52}$$

$$|\mathcal{M}(s_R\bar{d}_R \to s_R\bar{d}_R)|^2 = \frac{2(4\pi)^2 u^2}{9}\left|\frac{\alpha_s}{t}+\alpha_s\tan^2\phi P_t^{F'}\right|^2 \tag{A53}$$

$$|\mathcal{M}(s_L\bar{d}_R \to s_L\bar{d}_R)|^2 = |\mathcal{M}(s_R\bar{d}_L \to s_R\bar{d}_L)|^2 = \frac{2(4\pi)^2 s^2}{9}\left|\frac{\alpha_s}{t} - \alpha_s P_t^{F'}\right|^2 \tag{A54}$$

$$|\mathcal{M}(u_L\bar{d}_L \to u_L\bar{d}_L)|^2 = \frac{2(4\pi)^2 u^2}{9}\left(\left|\frac{\alpha_s}{t} + \frac{2\kappa}{3}P_t^F + \alpha_s\cot^2\phi P_t^{F'}\right|^2\right) \tag{A55}$$

$$|\mathcal{M}(u_R\bar{d}_R \to u_R\bar{d}_R)|^2 = \frac{2(4\pi)^2 u^2}{9}\left|\frac{\alpha_s}{t} + \alpha_s\tan^2\phi P_t^{F'}\right|^2 \tag{A56}$$

$$|\mathcal{M}(u_L\bar{d}_R \to u_L\bar{d}_R)|^2 = |\mathcal{M}(u_r\bar{d}_L \to u_R\bar{d}_L)|^2 = \frac{2(4\pi)^2 s^2}{9}\left|\frac{\alpha_s}{t} - \alpha_s P_t^{F'}\right|^2 \tag{A57}$$

$$|\mathcal{M}(u_L\bar{s}_L \to u_L\bar{s}_L)|^2 = \frac{2(4\pi)^2 u^2}{9}\left(\left|\frac{\alpha_s}{t} - \frac{\kappa}{3}P_t^F + \alpha_s\cot^2\phi P_t^{F'}\right|^2\right) \tag{A58}$$

$$|\mathcal{M}(u_R\bar{s}_R \to u_R\bar{s}_R)|^2 = \frac{2(4\pi)^2 u^2}{9}\left|\frac{\alpha_s}{t} + \alpha_s\tan^2\phi P_t^{F'}\right|^2 \tag{A59}$$

$$|\mathcal{M}(u_L\bar{s}_R \to u_L\bar{s}_R)|^2 = |\mathcal{M}(u_R\bar{s}_L \to u_R\bar{s}_L)|^2 = \frac{2(4\pi)^2 s^2}{9}\left|\frac{\alpha_s}{t} - \alpha_s P_t^{F'}\right|^2. \tag{A60}$$

[1] S. Dimopolous and L. Susskind, Nucl. Phys. **B155**, 237 (1979); E. Eitchen and K. Lane, Phys. Lett. **90B**, 125 (1980).

[2] S. Weinberg, Phys. Rev. D **19**, 1277 (1979); L. Suskind, *ibid.* **20**, 2619 (1979); E. Farhi and L. Susskind, Phys. Rep. **74**, 277 (1981).

[3] Y. Nambu, in *Proceedings of the XI Warsaw Symposium on Elementary Particle Physics*, edited by Z. Adjuk *et al.* (World Scientific, Singapore, 1989); V. A. Miransky, M. Tanabashi, and M. Yamawaki, Phys. Lett. B **221**, 177 (1989); R. R. Mendel and V. A. Miransky, *ibid.* **268**, 384 (1991); W. A. Bardeen, C. T. Hill, and M. Lindner, Phys. Rev. D **41**, 1647 (1990).

[4] C. T. Hill, Phys. Lett. B **345**, 483 (1995).

[5] S. F. King, Phys. Rev. D **45**, 990 (1992).

[6] B. Dobrescu and C. T. Hill, Phys. Rev. Lett. **81**, 2634 (1998); R. S. Chivukula, B. A. Dobrescu, H. Georgi, and C. T. Hill, Phys. Rev. D **59**, 075003 (1999).

[7] A top-flavor version can be found in H.-J. He, T. M. P. Tait, and C.-P. Yuan, Phys. Rev. D **62**, 011702(R) (2000).

[8] G. Burdman and N. Evans, Phys. Rev. D **59**, 115005 (1999).

[9] R. S. Chivukula and H. Georgi, Phys. Lett. B **188**, 99 (1987).

[10] H. Georgi, in *Proceedings of the 1990 International Workshop On Strong Coupling Gauge Theories And Beyond*, edited by T. Muta and K. Yamawaki (World Scientific, Singapore, 1991);

Nucl. Phys. **B416**, 699 (1994).

[11] R. S. Chivukula and J. Terning, Phys. Lett. B **385**, 209 (1996).

[12] G. Burdman, R. S. Chivukula, and N. Evans, Phys. Rev. D **61**, 035009 (2000).

[13] R. S. Chivukula, A. G. Cohen, and E. H. Simmons, Phys. Lett. B **380**, 92 (1996).

[14] Y. Nambu and G. Jona-Lasinio, Phys. Rev. **122**, 345 (1961).

[15] E. H. Simmons, Phys. Rev. D **55**, 1678 (1997).

[16] I. Bertram and E. H. Simmons, Phys. Lett. B **443**, 347 (1998).

[17] D0 Collaboration, B. Abbott *et al.*, Phys. Rev. Lett. **82**, 2457 (1999).

[18] CDF Collaboration, P. Koehn, in Proceedings International Europhysics Conference on High-Energy Physics (EPS-HEP 99), Tampere, Finland, 1999.

[19] T. Stelzer, Z. Sullivan, and S. Willenbrock, Phys. Rev. D **58**, 094021 (1998).

[20] L. Randall, Nucl. Phys. **B403**, 122 (1993).

[21] S. C. Bennett and C. E. Wieman, Phys. Rev. Lett. **82**, 2484 (1999).

[22] Particle Data Group, C. Caso *et al.*, Eur. Phys. J. C **3**, 1 (1998). The most recent value of $Q_W(Cs)$ can be found in the 1999 update of the PDG at http://pdg.lbl.gov.